# Deep Learning of Vortex Induced Vibrations

**M. Raissi[1]†, Z. Wang[2], M. S. Triantafyllou[2], and G. E. Karniadakis[1]**

[1]Division of Applied Mathematics, Brown University, Providence, RI 02912, USA

[2]Department of Mechanical Engineering, Massachusetts Institute of Technology, Cambridge, MA 02139, USA

Vortex induced vibrations of bluff bodies occur when the vortex shedding frequency is close to the natural frequency of the structure. Of interest is the prediction of the lift and drag forces on the structure given some limited and scattered information on the velocity field. This is an inverse problem that is not straightforward to solve using standard computational fluid dynamics (CFD) methods, especially since no information is provided for the pressure. An even greater challenge is to infer the lift and drag forces given some dye or smoke visualizations of the flow field. Here we employ deep neural networks that are extended to encode the incompressible Navier-Stokes equations coupled with the structure's dynamic motion equation. In the first case, given scattered data in space-time on the the velocity field and the structure's motion, we use four coupled deep neural networks to infer very accurately the structural parameters, the entire time-dependent pressure field (with no prior training data), and reconstruct the velocity vector field and the structure's dynamic motion. In the second case, given scattered data in space-time on a concentration field only, we use five coupled deep neural networks to infer very accurately the vector velocity field and all other quantities of interest as before. This new paradigm of inference in fluid mechanics for coupled multi-physics problems is part of our ongoing development of *physics-informed learning machines*, where the traditional CFD methodology is abandoned in favor of deep neural networks inference, circumventing the tyranny of elaborate mesh generation.

## 1. Introduction

Fluid-structure interactions (FSI) are omnipresent in engineering applications (Paidoussis 1998, 2004), e.g. in long pipes carrying fluids, in heat exchangers, in wind turbines, in gas turbines, in oil platforms and long risers for deep sea drilling. Vortex induced vibrations (VIV), in particular, are a special class of fluid-structure interactions (FSI), which involve a resonance condition. They are caused in external flows past bluff bodies when the frequency of the shed vortices from the body is close to the natural frequency of the structure (Williamson & Govardhan 2004). A prototypical example is flow past a circular cylinder that involves the so-called von Kármán shedding with a non-dimensional frequency (Strouhal number) of about 0.2. If the cylinder is elastically mounted, its resulting motion is caused by the lift force and the drag force in the crossflow and streamwise directions, respectively, and can reach about $1D$ and $0.1D$ in amplitude, where $D$ is the cylinder diameter. Clearly, for large structures like a long riser in deep sea drilling, this is a very large periodic motion that will lead to fatigue and hence a short life time for the structure.

Using traditional computational fluid dynamics (CFD) methods we can predict accurately VIV (Evangelinos & Karniadakis (1999)), both the flow field and the structure's

† Email address for correspondence: maziar_raissi@brown.edu

motion. However, CFD simulations are limited to relatively low Reynolds numbers and simple geometric configurations and involve the generation of elaborate and moving grids that may need to be updated frequently. Moreover, some of the structural characteristics, e.g. damping, are not readily available and hence separate experiments are required to obtain such quantities involved in CFD modeling of FSI. Solving inverse coupled CFD problems, however, is typically computationally prohibitive and often requires the solution of ill-posed problems. For the vibrating cylinder problem, in particular, we may have available data for the motion of the cylinder or some limited noisy measurements of the velocity field in the wake or some flow visualizations obtained by injecting dye upstream for liquid flows or smoke for air flows. Of interest is to determine the forces on the body that will determine the dynamic motion and possibly deformation of the body, and ultimately its fatigue life for safety evaluations.

In this work, we take a different approach building on our previous work on physics informed deep learning (Raissi *et al.* 2017*d*,*c*) and extending this concept to coupled multi-physics problems. Instead of solving the fluid mechanics equations and the dynamic equation for the motion of the structure using numerical discretization, we learn the velocity and pressure fields and the structure's motion using coupled deep neural networks with scattered data in space-time as input. The governing equations are employed as part of the loss function and play the role of regularization mechanisms. Hence, experimental input that may be noisy and at scattered spatio-temporal locations can be readily utilized in this new framework. Moreover, as we have shown in previous work, *physics informed neural networks* are particularly effective in solving inverse problems and discovering the hidden physics of coupled multi-physics problems (Raissi 2018*a*).

The paper is organized as follows. In the next section, we give an overview of the proposed algorithm, set up the problem and describe the synthetic data that we generate to test the performance of the method. In section §3 we present the results for three cases. We start with a pedagogical example by assuming that we know the forces on the body and we seek to obtain the structure's motion without solving explicitly the equation of motion. We then consider a case where we know the velocity field and the motion at some scattered data in space-time and we infer the lift and drag forces while at the same time we learn the pressure field and the entire velocity field and dynamic motion. We then consider an even more interesting case where we only assume available concentration data in space-time and from that information we obtain all the flow fields and motion as well as the lift and drag forces. We conclude with a short summary.

## 2. Problem Setup and Solution Methodology

We begin by considering the prototype VIV problem of flow past a circular cylinder. The fluid motion is governed by the incompressible Navier-Stokes equations while the dynamics of the structure is described in a general form involving displacement, velocity, and acceleration terms. In particular, let us consider the two-dimensional version of flow over a flexible cable, i.e., an elastically mounted cylinder (Bourguet *et al.* 2011). The two-dimensional problem contains most of the salient features of the three-dimensional case and consequently it is relatively straightforward to generalize the proposed framework to the flexible cylinder/cable problem. In two dimensions, the physical model of the cable reduces to a mass-spring-damper system. There are two directions of motion for the cylinder: the streamwise (i.e., $x$) direction and the crossflow (i.e., $y$) direction. In this work, we assume that the cylinder can only move in the crossflow (i.e., $y$) direction; we concentrate on crossflow vibrations since this is the primary VIV direction. However, it is a simple extension to study cases where the cylinder is free to move in both

streamwise and crossflow directions. The cylinder displacement is defined by the variable $\eta$ corresponding to the crossflow motion. The equation of motion for the cylinder is then given by

$$\rho\eta_{tt} + b\eta_t + k\eta = f_L, \tag{2.1}$$

where $\rho$, $b$, and $k$ are the mass, damping, and stiffness parameters, respectively. The fluid lift force on the structure is denoted by $f_L$. The mass $\rho$ of the cylinder is usually a known quantity; however, the damping $b$ and the stiffness $k$ parameters are often unknown in practice. In the current work, we put forth a deep learning approach for estimating these parameters from measurements. We start by assuming that we have access to the input-output data $\{t^n, \eta^n\}_{n=1}^N$ and $\{t^n, f_L^n\}_{n=1}^N$ on the displacement $\eta(t)$ and the lift force $f_L(t)$ functions, respectively. Having access to direct measurements of the forces exerted by the fluid on the structure is obviously a strong assumption. However, we start with this simpler but pedagogical case and we will relax this assumption later in this section.

Inspired by recent developments in *physics informed deep learning* (Raissi *et al.* 2017*d*,*c*) and *deep hidden physics models* (Raissi 2018*a*), we propose to approximate the unknown function $\eta$ by a deep neural network. This choice is motivated by modern techniques for solving forward and inverse problems involving partial differential equations, where the unknown solution is approximated either by a neural network (Raissi *et al.* 2017*d*,*c*; Raissi 2018*a*,*b*; Raissi *et al.* 2018*a*) or a Gaussian process (Raissi *et al.* 2018*b*; Raissi & Karniadakis 2018; Raissi *et al.* 2017*a*,*b*; Raissi 2017; Perdikaris *et al.* 2017; Raissi & Karniadakis 2016). Moreover, placing a prior on the solution is fully justified by similar approaches pursued in the past centuries by classical methods of solving partial differential equations such as finite elements, finite differences, or spectral methods, where one would expand the unknown solution in terms of an appropriate set of basis functions. Approximating the unknown function $\eta$ by a deep neural network and using equation (2.1) allow us to obtain the following *physics-informed neural network*

$$f_L := \rho\eta_{tt} + b\eta_t + k\eta. \tag{2.2}$$

It worth noting that the damping $b$ and the stiffness $k$ parameters turn into parameters of the resulting physics informed neural network $f_L$. We obtain the required derivatives to compute the residual network $f_L$ by applying the chain rule for differentiating compositions of functions using automatic differentiation (Baydin *et al.* 2015). Automatic differentiation is different from, and in several respects superior to, numerical or symbolic differentiation – two commonly encountered techniques of computing derivatives. In its most basic description (Baydin *et al.* 2015), automatic differentiation relies on the fact that all numerical computations are ultimately compositions of a finite set of elementary operations for which derivatives are known. Combining the derivatives of the constituent operations through the chain rule gives the derivative of the overall composition. This allows accurate evaluation of derivatives at machine precision with ideal asymptotic efficiency and only a small constant factor of overhead. In particular, to compute the required derivatives we rely on Tensorflow (Abadi *et al.* 2016), which is a popular and relatively well documented open source software library for automatic differentiation and deep learning computations.

The shared parameters of the neural networks $\eta$ and $f_L$, in addition to the damping $b$ and the stiffness $k$ parameters, can be learned by minimizing the following sum of squared errors loss function

$$\sum_{n=1}^{N} |\eta(t^n) - \eta^n|^2 + \sum_{n=1}^{N} |f_L(t^n) - f_L^n|^2. \tag{2.3}$$

The first summation in this loss function corresponds to the training data on the displacement $\eta(t)$ while the second summation enforces the dynamics imposed by equation (2.1).

### 2.1. *Inferring Lift and Drag Forces from Velocity Measurements*

So far, we have been operating under the assumption that we have access to direct measurements of the lift force $f_L$. In the following, we are going to relax this assumption by recalling that the fluid motion is governed by the incompressible Navier-Stokes equations given explicitly by

$$\begin{aligned} &u_t + uu_x + vu_y = -p_x + Re^{-1}(u_{xx} + u_{yy}),\\ &v_t + uv_x + vv_y = -p_y + Re^{-1}(v_{xx} + v_{yy}) - \eta_{tt},\\ &u_x + v_y = 0. \end{aligned} \tag{2.4}$$

Here, $u(t, x, y)$ and $v(t, x, y)$ are the streamwise and crossflow components of the velocity field, respectively, while $p(t, x, y)$ denotes the pressure, and $Re$ is the Reynolds number based on the cylinder diameter and the free stream velocity. We consider the incompressible Navier-Stokes equations in the coordinate system attached to the cylinder, so that the cylinder appears stationary in time. This explains the appearance of the extra term $\eta_{tt}$ in the second momentum equation (2.4). The second VIV learning problem is defined as follows: Given measurements $\{t^n, x^n, y^n, u^n, v^n\}_{n=1}^N$ of the velocity field† in addition to the data $\{t^n, \eta^n\}_{n=1}^N$ on the displacement and knowing the dynamics of the fluid (2.4), we are interested in reconstructing the velocity field as well as the pressure.

We proceed by approximating $u(t, x, y)$, $v(t, x, y)$, $p(t, x, y)$, and $\eta(t)$ by four neural networks. This prior assumption along with the incompressible Navier-Stokes equations (2.4) result into the following *physics-informed neural networks*

$$\begin{aligned} &e_1 := u_t + uu_x + vu_y + p_x - Re^{-1}(u_{xx} + u_{yy}),\\ &e_2 := v_t + uv_x + vv_y + p_y - Re^{-1}(v_{xx} + v_{yy}) + \eta_{tt},\\ &e_3 := u_x + v_y. \end{aligned} \tag{2.5}$$

We use automatic differentiation (Baydin *et al.* 2015) to obtain the required derivatives to compute the residual networks $e_1$, $e_2$, and $e_3$. The shared parameters of the neural networks $u$, $v$, $p$, $\eta$, $e_1$, $e_2$, and $e_3$ can be learned by minimizing the sum of squared errors loss function

$$\begin{aligned} &\textstyle\sum_{n=1}^N \left(|u(t^n, x^n, y^n) - u^n|^2 + |v(t^n, x^n, y^n) - v^n|^2\right)\\ &+ \textstyle\sum_{n=1}^N |\eta(t^n) - \eta^n|^2 + \sum_{i=1}^3 \sum_{n=1}^N \left(|e_i(t^n, x^n, y^n)|^2\right). \end{aligned} \tag{2.6}$$

Here, the first two summations correspond to the training data on the fluid velocity and the structure displacement while the last summation enforces the dynamics imposed by equation (2.4).

The fluid forces on the cylinder are functions of the pressure and the velocity gradients. Consequently, having trained the neural networks, we can use

$$F_D = \oint \left[-pn_x + 2Re^{-1}u_x n_x + Re^{-1}\left(u_y + v_x\right)n_y\right] ds, \tag{2.7}$$

$$F_L = \oint \left[-pn_y + 2Re^{-1}v_y n_y + Re^{-1}\left(u_y + v_x\right)n_x\right] ds, \tag{2.8}$$

† Take for example the case of reconstructing a flow field from scattered measurements obtained from Particle Image Velocimetry (PIV) or Particle Tracking Velocimetry (PTV).

to obtain the lift and drag forces exerted by the fluid on the cylinder. Here, $(n_x, n_y)$ is the outward normal on the cylinder and $ds$ is the arc length on the surface of the cylinder. We use the trapezoidal rule to approximately compute these integrals, and we use equation (2.8) to obtain the required data on the lift force. These data are then used to estimate the structural parameters $b$ and $k$ by minimizing the loss function (2.3).

### 2.2. *Inferring Lift and Drag Forces from Flow Visualizations*

We now consider the second VIV learning problem by taking one step further and circumvent the need for having access to measurements of the velocity field by leveraging the following equation

$$c_t + uc_x + vc_y = Pe^{-1}(c_{xx} + c_{yy}), \tag{2.9}$$

governing the evolution of the concentration $c(t, x, y)$ of a passive scalar injected into the fluid flow dynamics described by the incompressible Navier-Stokes equations (2.4). Here, $Pe$ denotes the Péclet number, defined based on the cylinder diameter, the free-stream velocity and the diffusivity of the concentration species. The second VIV learning problem is defined as follows: Given scattered and noisy measurements $\{t^n, x^n, y^n, c^n\}_{n=1}^N$ of the concentration $c(t, x, y)$ of the passive scalar in space-time, we are interested in inferring the latent (hidden) quantities $u(t, x, y)$, $v(t, x, y)$, and $p(t, x, y)$. Consequently, equations (2.7) and (2.8) enable us to compute the drag and lift forces, respectively, as functions of the inferred pressure and velocity gradients.

In addition to approximating $u(t, x, y)$, $v(t, x, y)$, $p(t, x, y)$, and $\eta(t)$ by four deep neural networks as before, we represent $c(t, x, y)$ by yet another neural network. This prior assumption along with equation (2.9) results in the following additional *physics informed neural network*

$$e_4 := c_t + uc_x + vc_y - Pe^{-1}(c_{xx} + c_{yy}). \tag{2.10}$$

The residual networks $e_1$, $e_2$, and $e_3$ are defined as before (see equation (2.5)). We use automatic differentiation (Baydin *et al.* 2015) to obtain the required derivatives to compute the additional residual network $e_4$. The shared parameters of the neural networks $c$, $u$, $v$, $p$, $\eta$, $e_1$, $e_2$, $e_3$, $e_4$ can be learned by minimizing the sum of squared errors loss function

$$\begin{aligned} &\textstyle\sum_{n=1}^N \left(|c(t^n, x^n, y^n) - c^n|^2 + |\eta(t^n) - \eta^n|^2\right) \\ &+ \textstyle\sum_{m=1}^M \left(|u(t^m, x^m, y^m) - u^m|^2 + |v(t^m, x^m, y^m) - v^m|^2\right) \\ &+ \textstyle\sum_{i=1}^4 \sum_{n=1}^N \left(|e_i(t^n, x^n, y^n)|^2\right). \end{aligned} \tag{2.11}$$

Here, the first summation corresponds to the training data on the concentration of the passive scalar and the structure's displacement, the second summation corresponds to the Dirichlet boundary data on the velocity field, and the last summation enforces the dynamics imposed by equations (2.4) and (2.9). Upon training, we use equation (2.8) to obtain the required data on the lift force. Such data are then used to estimate the structural parameters $b$ and $k$ by minimizing the loss function (2.3).

## 3. Results†

To generate a high-resolution dataset for the VIV problem we have performed direct numerical simulations (DNS) employing the high-order spectral-element method (Kar-

† All data and codes used in this manuscript will be publicly available on GitHub at https://github.com/maziarraissi/DeepVIV.

niadakis & Sherwin 2005), together with the coordinate transformation method to take account of the boundary deformation (Newman & Karniadakis 1997). The computational domain is $[-6.5\,D, 23.5\,D]\times[-10\,D, 10\,D]$, consisting of 1,872 quadrilateral elements. The cylinder center was placed at $(0, 0)$. On the inflow, located at $x/D = -6.5$, we prescribe $(u = U_\infty, v = 0)$. On the outflow, where $x/D = 23.5$, zero-pressure boundary condition $(p = 0)$ is imposed. On both top and bottom boundaries where $y/D = \pm 10$, a periodic boundary condition is used. The Reynolds number is $Re = 100$, $\rho = 2$, $b = 0.084$ and $k = 2.2020$. For the case with dye, we assumed the Péclet number $Pe = 90$. First, the simulation is carried out until $t = 1000\,\frac{D}{U_\infty}$ when the system is in steady periodic state. Then, an additional simulation for $\Delta t = 14\,\frac{D}{U_\infty}$ is performed to collect the data that are saved in 280 field snapshots. The time interval between two consecutive snapshots is $\Delta t = 0.05\frac{D}{U_\infty}$. Note here $D = 1$ is the diameter of the cylinder and $U_\infty = 1$ is the inflow velocity. We use the DNS results to compute the lift and drag forces exerted by the fluid on the cylinder.

To illustrate the effectiveness of our approach, let us start with two time series consisting of $N = 111$ observations of the displacement and the lift force. These data correspond to damping and stiffness parameters with exact values $b = 0.084$ and $k = 2.2020$, respectively. Here, the cylinder is assumed to have a mass of $\rho = 2.0$. This data-set is then used to train a 10-layer deep neural network with 32 neurons per hidden layers by minimizing the sum of squared errors loss function (2.3) using the Adam optimizer (Kingma & Ba 2014). Upon training, the network is used to predict the entire solution functions $\eta(t)$ and $f_L(t)$, as well as the unknown structural parameters $b$ and $k$. In addition to almost perfect reconstructions of the two time series for displacement and lift force, the proposed framework is capable of identifying the correct values for the structural parameters $b$ and $k$ with remarkable accuracy. The learned values for the damping and stiffness parameters are $b = 0.08438281$ and $k = 2.2015007$. This corresponds to around 0.45% and 0.02% relative errors in the estimated values for $b$ and $k$, respectively.

In general, the choice of a neural network's architecture (e.g., number of layers and neurons) is crucial and in many cases still remains an art that relies on one's ability to balance the trade off between *expressivity* and *trainability* of the neural network (Raghu *et al.* 2016). Our empirical findings so far indicate that deeper and wider networks are usually more expressive (i.e., they can capture a larger class of functions) but are often more costly to train (i.e., a feed-forward evaluation of the neural network takes more time and the optimizer requires more iterations to converge). However, these observations should be interpreted as a conjecture rather as firm results†. In this work, we have tried to choose the neural networks' architectures in a consistent fashion throughout the manuscript by setting the number of layers to 10 and the number of neurons to 32. Consequently, there might exist other architectures that improve some of the results reported in the current work.

Let us now consider the case where we do not have access to direct measurements of the lift force $f_L$. In this case, we can use measurements of the velocity field, obtained for instance via Particle Image Velocimetry (PIV) or Particle Tracking Velocimetry (PTV), to reconstruct the velocity field, the pressure, and consequently the drag and lift forces. A representative snapshot of the data on the velocity field is depicted in the top left and top middle panels of figure 1. The neural network architectures used here consist of 10 layers

† We encourage the interested reader to check out the codes corresponding to this paper on GitHub at https://github.com/maziarraissi/DeepVIV and experiment with different choices for the neural networks' architectures.

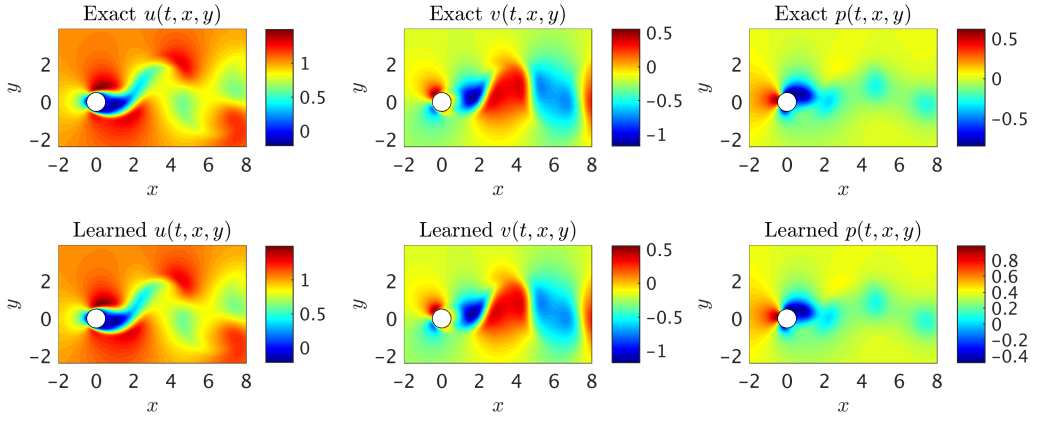


FIGURE 1. *Vortex Induced Vibrations (Velocity Measurements)*: A representative snapshot of the data on the velocity field is depicted in the top left and top middle panels of this figure. The algorithm is capable of accurately (of the order of $10^{-3}$) reconstructing the velocity field and more importantly the pressure without having access to even a single observation on the pressure itself.

with 32 neurons in each hidden layer. A summary of our results is presented in figure 1. The proposed framework is capable of accurately (of the order of $10^{-3}$) reconstructing the velocity field; however, a more intriguing result stems from the network's ability to provide an accurate prediction of the entire pressure field $p(t,x,y)$ in the absence of any training data on the pressure itself. A visual comparison against the exact pressure is presented in figure 1 for a representative snapshot of the pressure. It is worth noticing that the difference in magnitude between the exact and the predicted pressure is justified by the very nature of incompressible Navier-Stokes equations, since the pressure field is only identifiable up to a constant. This result of inferring a continuous quantity of interest from auxiliary measurements by leveraging the underlying physics is a great example of the enhanced capabilities that our approach has to offer, and highlights its potential in solving high-dimensional inverse problems.

The trained neural networks representing the velocity field and the pressure can be used to compute the drag and lift forces by employing equations (2.7) and (2.8), respectively. The resulting drag and lift forces are compared to the exact ones in figure 2. In the following, we are going to use the computed lift force to generate the required training data on $f_L$ and estimate the structural parameters $b$ and $k$ by minimizing the loss function (2.3). Upon training, the proposed framework is capable of identifying the correct values for the structural parameters $b$ and $k$ with remarkable accuracy. The learned values for the damping and stiffness parameters are $b = 0.0844064$ and $k = 2.1938791$. This corresponds to around 0.48% and 0.37% relative errors in the estimated values for $b$ and $k$, respectively.

Let us continue with the case where we do not have access to direct observations of the lift force $f_L$. This time rather than using data on the velocity field, we use measurements of the concentration of a passive scalar (e.g., dye or smoke) injected into the system. In the following, we are going to employ such data to reconstruct the velocity field, the pressure, and consequently the drag and lift forces. A representative snapshot of the data on the concentration of the passive scalar is depicted in the top left panel of figure 3. The neural networks' architectures used here consist of 10 layers with 32 neurons per each hidden layer. A summary of our results is presented in figure 3. The proposed framework is capable of accurately (of the order of $10^{-3}$) reconstructing the concentration. However, a

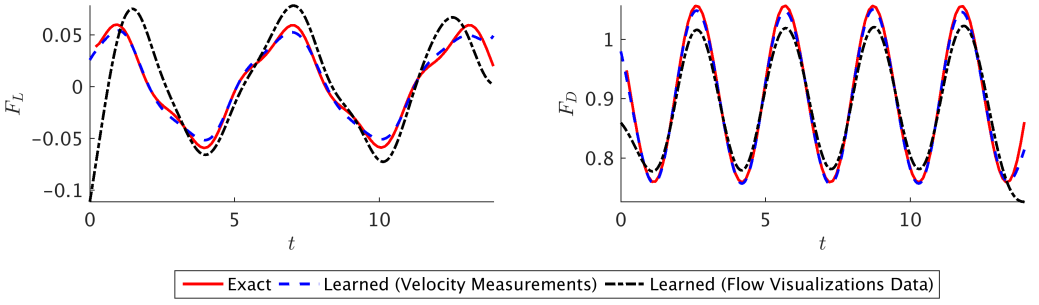


FIGURE 2. *Vortex Induced Vibrations (Lift and Drag Forces)*: In this figure, the resulting lift (left) and drag (right) forces are compared to the exact ones. The red solid lines correspond to the exact lift and drag forces. The blue dashed lines represent the learned fluid forces using the velocity measurements, while the black dotted lines correspond to the learned lift and drag forces obtained by using the flow visualization data.

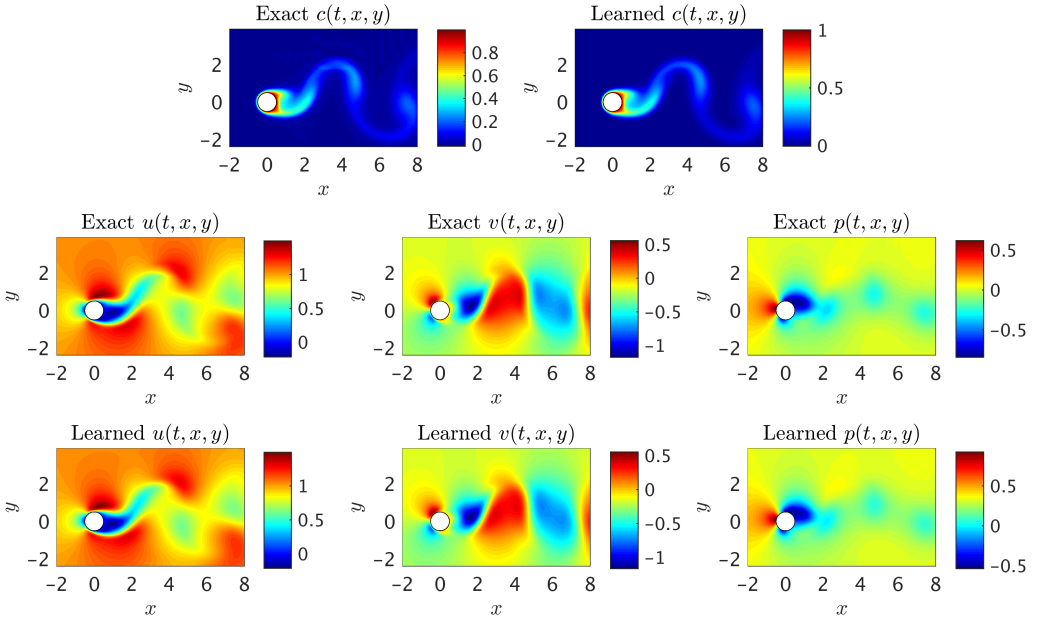


FIGURE 3. *Vortex Induced Vibrations (Flow Visualizations Data)*: A representative snapshot of the data on the concentration of the passive scalar is depicted in the top left panel of this figure. The algorithm is capable of accurately (of the order of $10^{-3}$) reconstructing the concentration of the passive scalar and more importantly the velocity field as well as the pressure without having access to enough observations of these quantities themselves.

truly intriguing result stems from the network's ability to provide an accurate prediction of the entire velocity vector field as well as the pressure, in the absence of sufficient training data on the pressure and the velocity field themselves. A visual comparison against the exact quantities is presented in figure 3 for a representative snapshot of the velocity field and the pressure. This result of inferring multiple hidden quantities of interest from auxiliary measurements by leveraging the underlying physics is a great example of the enhanced capabilities that *physics-informed deep learning* has to offer, and highlights its potential in solving high-dimensional inverse problems.

Following the same procedure as in the previous example, the trained neural networks representing the velocity field and the pressure can be used to compute the drag and

lift forces by employing equations (2.7) and (2.8), respectively. The resulting drag and lift forces are compared to the exact ones in figure 2. In the following, we are going to use the computed lift force to generate the required training data on $f_L$ and estimate the structural parameters $b$ and $k$ by minimizing the loss function (2.3). Upon training, the proposed framework is capable of identifying the correct values for the structural parameters $b$ and $k$ with surprising accuracy. The learned values for the damping and stiffness parameters are $b = 0.08600664$ and $k = 2.2395933$. This corresponds to around 2.39% and 1.71% relative errors in the estimated values for $b$ and $k$, respectively.

## 4. Summary

We have considered the classical coupled problem of a freely vibrating cylinder due to lift forces and demonstrated how deep learning can be used to infer quantities of interest from scattered data in space-time. In the *first VIV learning problem*, we inferred the pressure field and structural parameters, and hence the lift and drag on the vibrating cylinder using velocity and displacement data in time-space. In the *second VIV learning problem*, we inferred the velocity and pressure fields as well as the structural parameters given data on a passive scalar in space-time. The framework we propose here represents a *paradigm shift* in fluid mechanics simulation as it uses the governing equations as regularization mechanisms in the loss function of the corresponding minimization problem. It is particularly effective for multi-physics problems as the coupling between fields can be readily accomplished by sharing parameters among the multiple neural networks – here 4 neural networks the first problem and 5 for the second one – and for more general coupled problems by also including coupled terms in the loss function. There are many questions that this new type of modeling raises, both theoretical and practical, e.g. efficiency, solution uniqueness, accuracy, etc. We have considered such questions here in the present context as well as in our previous work in the context of physics-informed learning machines but admittedly at the present time it is not possible to rigorously answer such questions. We hope, however, that our present work will ignite interest in physics-informed deep learning that can be used effectively for many different fields of multi-physics fluid mechanics.

## Acknowledgements

This work received support by the DARPA EQUiPS grant N66001-15-2-4055 and the AFOSR grant FA9550-17-1-0013.

## REFERENCES

Abadi, M., Agarwal, A., Barham, P., Brevdo, E., Chen, Z., Citro, C., Corrado, G. S., Davis, A., Dean, J., Devin, M. & others 2016 Tensorflow: Large-scale machine learning on heterogeneous distributed systems. *arXiv preprint arXiv:1603.04467* .

Baydin, A. G., Pearlmutter, B. A., Radul, A. A. & Siskind, J. M. 2015 Automatic differentiation in machine learning: a survey. *arXiv preprint arXiv:1502.05767* .

Bourguet, R., Karniadakis, G. E. & Triantafyllou, M. S. 2011 Vortex-induced vibrations of a long flexible cylinder in shear flow. *Journal of Fluid Mechanics* **677**, 342–382.

Evangelinos, C. & Karniadakis, G. E. 1999 Dynamics and flow structures in the turbulent wake of rigid and flexible cylinders subject to vortex-induced vibrations. *Journal of Fluid Mechanics* **400**, 91–124.

Karniadakis, G. E. & Sherwin, S. 2005 *Spectral/hp Element Methods for Computational Fluid Dynamics, 2nd edition*. Oxford,UK: Oxford University Press.

Kingma, D. P. & Ba, J. 2014 Adam: A method for stochastic optimization. *arXiv preprint arXiv:1412.6980* .

Newman, D. J. & Karniadakis, G. E. 1997 A direct numerical simulation study of flow past a freely vibrating cable. *Journal of Fluid Mechanics* **344**, 95–136.

Paidoussis, M. P. 1998 *fluid-Structure Interactions: Slender Structures and Axial Flow volume 1*. Academic Press.

Paidoussis, M. P. 2004 *fluid-structure Interactions: Slender Structures and Axial Flow volume 2*. Academic Press.

Perdikaris, P., Raissi, M., Damianou, A., Lawrence, N. D. & Karniadakis, G. E. 2017 Nonlinear information fusion algorithms for data-efficient multi-fidelity modelling. *Proc. R. Soc. A* **473** (2198), 20160751.

Raghu, M., Poole, B., Kleinberg, J., Ganguli, S. & Sohl-Dickstein, J. 2016 On the expressive power of deep neural networks. *arXiv preprint arXiv:1606.05336* .

Raissi, M. 2017 Parametric Gaussian process regression for big data. *arXiv preprint arXiv:1704.03144* .

Raissi, M. 2018*a* Deep hidden physics models: Deep learning of nonlinear partial differential equations. *arXiv preprint arXiv:1801.06637* .

Raissi, M. 2018*b* Forward-backward stochastic neural networks: Deep learning of high-dimensional partial differential equations. *arXiv preprint arXiv:1804.07010* .

Raissi, M. & Karniadakis, G. 2016 Deep multi-fidelity Gaussian processes. *arXiv preprint arXiv:1604.07484* .

Raissi, M. & Karniadakis, G. E. 2018 Hidden physics models: Machine learning of nonlinear partial differential equations. *Journal of Computational Physics* **357**, 125–141.

Raissi, M., Perdikaris, P. & Karniadakis, G. E. 2017*a* Inferring solutions of differential equations using noisy multi-fidelity data. *Journal of Computational Physics* **335**, 736–746.

Raissi, M., Perdikaris, P. & Karniadakis, G. E. 2017*b* Machine learning of linear differential equations using Gaussian processes. *Journal of Computational Physics* **348**, 683 – 693.

Raissi, M., Perdikaris, P. & Karniadakis, G. E. 2017*c* Physics informed deep learning (part I): Data-driven solutions of nonlinear partial differential equations. *arXiv preprint arXiv:1711.10561* .

Raissi, M., Perdikaris, P. & Karniadakis, G. E. 2017*d* Physics informed deep learning (part II): Data-driven discovery of nonlinear partial differential equations. *arXiv preprint arXiv:1711.10566* .

Raissi, M., Perdikaris, P. & Karniadakis, G. E. 2018*a* Multistep neural networks for data-driven discovery of nonlinear dynamical systems. *arXiv preprint arXiv:1801.01236* .

Raissi, M., Perdikaris, P. & Karniadakis, G. E. 2018*b* Numerical gaussian processes for time-dependent and nonlinear partial differential equations. *SIAM Journal on Scientific Computing* **40** (1), A172–A198.

Williamson, C. H. K. & Govardhan, R. 2004 Vortex-induced vibration. *Annual Review of Fluid Mechanics* **36**, 413–455.